

# Study on fault line detection methods based on multi-feature fusion in distribution systems

Jiawei Yuan<sup>1</sup> | Zaibin Jiao<sup>1</sup> | Guang Feng<sup>2</sup> | Ming Chen<sup>2</sup> | Mingming Xu<sup>2</sup>

<sup>1</sup> School of Electrical Engineering, Xi'an Jiaotong University, Xi'an, China

<sup>2</sup> State Grid Henan Electric Power Research Institute, Zhengzhou, Henan, China

## Correspondence

Zaibin Jiao, School of Electrical Engineering, Xi'an Jiaotong University, Xi'an 710049, China.  
Email: jiaozaibin@mail.xjtu.edu.cn

## Abstract

Faulted line detection is used for locating faults and restoring service after the occurrence of a single line-to-ground fault in a non-effectively earthed network. The traditional single faulted line detection method cannot adapt to the fault diagnosis of distribution systems under unfavourable conditions, while faulted line selection schemes based on neural network have poor generalisation ability when the structure of distribution network changes. A novel faulted line detection method based on multi-feature integration is proposed to overcome the shortcomings of the previous methods. This study classifies the different fault characteristics of single line-to-ground faults in distribution systems, and analyses the applicable range of existing methods under multiple fault conditions. Subsequently, three detection methods that can be applied to different fault conditions and have complementarity are employed for feature extraction. Moreover, the extracted features of a feeder are processed by introducing the fault features of the remaining feeders, and the processed features are fused based on the fuzzy theory. Considering the selection of fault measure functions and weight coefficients in the fuzzy theory based on experience, an adaptive-network-based fuzzy inference system is employed for feature fusion. PSCAD and RTDS experiments confirmed the superior generalisation ability of the proposed method.

## 1 | INTRODUCTION

Non-effectively earthed networks are widely used in medium-voltage and low-voltage distribution systems. The stability of the network is influenced by various faults, among which single line-to-ground (SLG) faults account for 80% of all faults [1]. Although neutral indirectly grounded systems are allowed to operate 1–2 h after the occurrence of SLG faults, the non-fault phase voltage will rise to a high level, which is harmful to the insulation of electrical equipment and the safe operation of power systems. Moreover, it is difficult to detect the faulted line due to the relatively low fault current, especially in distribution systems with high-impedance grounding. Therefore, it is necessary to study faulted line detection methods to prevent a further deterioration of the fault.

Accordingly, faulted line detection techniques have been studied extensively in the past few decades. They can be

roughly divided into three groups: injected-current signal-based algorithms [2], single-feature-based algorithms [3–4], and multi-feature-based algorithms [5–9]. In [2], a thyristor used for detection was inserted into the secondary (delta) winding of a potential transformer. However, the additional equipment and the changes in the system structure limit its applications. Single-feature-based algorithms can be subdivided into two types: steady-state component-based methods [3] and transient-signal-based methods [4]. However, these methods are significantly affected by the network structure, complex fault situation, and electromagnetic interference, causing detection failures. Recently, several scholars have begun to apply modern information fusion technologies to detect the faulty feeder in distribution systems, and consequently, numerous methods have emerged. The wavelet transform method, zero-sequence active component method, and fifth-order harmonic current method were integrated to improve the accuracy of

This is an open access article under the terms of the [Creative Commons Attribution](https://creativecommons.org/licenses/by/4.0/) License, which permits use, distribution and reproduction in any medium, provided the original work is properly cited.

© 2020 The Authors. *IET Generation, Transmission & Distribution* published by John Wiley & Sons Ltd on behalf of The Institution of Engineering and Technology

fault line detection based on a genetic artificial neural network in [5]. Based on the fuzzy theory, the energy method and harmonic method were combined with wavelet analysis in [6]. In [7], decaying DC component (DDCC), transient energy, and reactive-power detection were used to describe the features of different fault conditions, and extenics were used for classification. The discrete wavelet transform was used for feature extraction, and the Bayesian selectivity technique was applied to identify the faulty feeder in [8]. However, the aforementioned methods used for feature extraction do not analyse the comprehensiveness and complementarity between different faulted line detection methods, leading to a lower reliability of identification under unfavourable conditions. In addition, a 1D convolutional neural network (CNN) was employed to extract the features of the data of each line and a neural network was used for feature fusion [9], mitigating the shortcomings of artificially designed criteria. However, prior-knowledge-based features are also concatenated as an input of the neural network, which shows that 1D CNN-based features are not sufficiently effective and have some limitations. Moreover, the structure and parameters are changed in the operation of distribution systems, and these special operation modes inevitably result in the invalidation of the fully connected and fixed input neural network.

In general, the existing faulted line detection methods show good performance for specific fault scenarios, but they may fail in other fault conditions. Consequently, comprehensive and complementary detection methods are used for feature extraction and effective intelligent algorithms are employed for feature fusion, as a possible approach toward faulted line detection. Most importantly, the generalisation ability of algorithms should be greatly emphasised.

This study classifies the different groups of SLG faults according to the fault characteristics in distribution systems with resonant grounding and analyses the applicable range of existing faulted line detection methods under the corresponding fault conditions, laying the foundation for the selection of comprehensive and complementary detection methods. Subsequently, the extracted features of a feeder using three detection methods are normalised by introducing the fault features of the remaining feeders, which makes it possible for faulty feeder identification when the structure of distribution network changes. The normalised features are fused based on the fuzzy theory, and an adaptive-network-based fuzzy inference system (ANFIS) is employed as an efficient and intelligent tool for feature fusion. As the data of each line are employed separately as input to the ANFIS, it is not necessary for the ANFIS-based method to retrain when the structure and parameters of the distribution systems change in routine operation. PSCAD and RTDS simulations demonstrate that the proposed method has strong generalisation ability and is suitable for an actual distribution system.

The rest of this paper is organised as follows. In Section 2, the classification of different fault conditions and the applicability of the existing detection methods are analysed. Section 3 presents the proposed method in detail. In Sections 4 and 5, the

superiority of the proposed method is verified and experimental results are discussed in detail. Section 6 concludes this paper.

## 2 | COMPLEMENTARY ANALYSIS OF DETECTION METHODS

### 2.1 | Classification of fault conditions

SLG faults occurring in a resonant earthed system can be roughly divided into low-impedance and high-impedance faults according to the grounding fault resistance. Moreover, high-impedance faults can be further classified into high-impedance underdamped fault and high-impedance overdamped fault [10]. Table 1 shows the corresponding equivalent circuit, its zero-sequence current, and its traditional current waveform for different fault types.

As shown in Table 1, the characteristics of the zero-sequence current between the fault and non-fault lines are considerably varied in the different fault conditions. With regard to the low-impedance fault, each line contains a large amount of high-frequency components. The zero-sequence current in the fault line is significantly different from the current in the sound lines, where the amplitude of the zero-sequence current in the fault line is the largest and the phase is opposite to that of the non-fault lines. For the high-impedance underdamped fault, the DDCC is evident in the fault line, whereas the sound lines contain few DDCC. However, there is no visible difference between the fault and non-fault lines regarding the high-impedance overdamped fault. Thus, the faulted line detection method should be selected according to the different fault types.

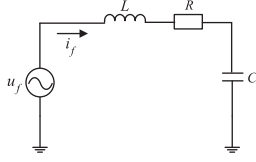
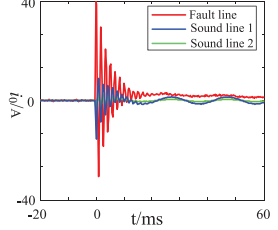
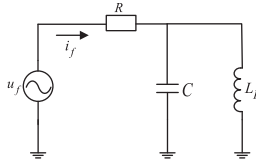
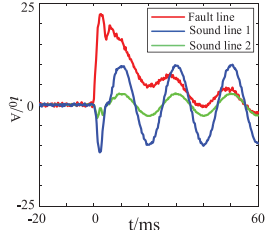
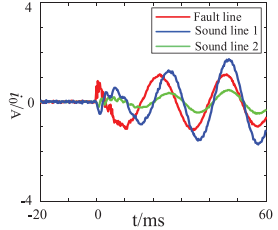
### 2.2 | Applicability analysis of detection methods

The applicability analysis of the existing detection methods is described in Table 2.

As shown in Table 2, a single faulted line detection method cannot be applied to all fault types. Therefore, some detection methods that can cover all fault types and complement each other should be selected. This study comprehensively considers the adaptability and complementarity of different detection methods, and consequently, it selects the transient current waveform synthesis (TCWS) method to identify low-impedance faults, the DDCC method to identify high-impedance underdamped faults, and the wavelet packet energy entropy (WPEE) method to identify high-impedance overdamped faults.

To summarise, this section classifies the zero-sequence current characteristics when SLG faults occur in a resonant earthed system and analyses the adaptability of existing detection methods to different fault types. Finally, three faulted line detection methods for multi-feature fusion are determined, and the detailed implementation will be introduced in the following section.

**TABLE 1** Study on the fault features of SLG faults in a resonant earthed system

Fault type	Equivalent circuit	Transient current	Current waveform
Low-impedance fault (I)		$i_f = U_m \omega_0 C \left[ \frac{1/LC}{\omega_0 \omega_f} \sin \varphi \sin \omega_f t + \frac{\delta}{\omega_f} \cos \varphi \sin \omega_f t - \cos \varphi \cos \omega_f t \right] e^{-\delta t} + U_m \omega_0 C \cos(\omega_0 t + \varphi)$	
High-impedance underdamped fault (II)		$i_f = (1 + L_p C p_1^2) A_1 e^{p_1 t} + (1 + L_p C p_2^2) A_2 e^{p_2 t} + (1 - \omega_0^2) B \sin(\omega_0 t + \varphi)$	
High-impedance overdamped fault (III)		$i_f = e^{-\delta t} [A_1 \cos(\omega_f t) + A_2 \sin(\omega_f t)] (1 + L_p C \delta^2) + B \sin(\omega_0 t + \varphi) (1 - L_p C \omega_0^2) - L_p C \{ 2\delta e^{-\delta t} [-\omega_f A_1 \sin(\omega_f t) + \omega_f A_2 \cos(\omega_f t)] \} + L_p C \{ e^{-\delta t} [-\omega_f^2 A_1 \cos(\omega_f t) - \omega_f^2 A_2 \sin(\omega_f t)] \}$	

**TABLE 2** Applicability analysis of detection methods

Detection method	Basic theory	Typical criteria	Applicability
Transient energy	The transient energy in a fault line is maximum [7]	$ \sum_{j=1}^n  W_j  -  W_i  / W_i  < 1$ [7]	I
Transient reactive power	The transient reactive power in a fault line is maximum [7]	$ \sum_{j=1}^n  Q_j  -  Q_i  / Q_i  < 1$ [7]	I
TCWS	There is a significant difference between the fault transient zero-sequence current waveforms of the fault feeder and the sound feeders [11]	<ol style="list-style-type: none"> <li>Calculating the corresponding energy of each sub-band signal and determining the predominant frequency band</li> <li>Calculating the correlation coefficient by sub-band coefficient</li> </ol> $\rho_{xy} = \frac{\sum_{n=0}^{N-1} x(n)y(n)}{[\sum_{n=0}^{N-1} x^2(n)y^2(n)]^{1/2}}, \rho_i = \frac{1}{N-1} \sum_{j=1, j \neq i}^N \rho_{ij}$ [11] <ol style="list-style-type: none"> <li>The line corresponding to the minimum <math>\rho</math> is identified as the faulty feeder</li> </ol>	I II
DDCC	The DDCC is large in the fault line, and small in the sound lines	The line corresponding to the maximum value of the DDCC is identified as the faulty feeder	II
WPEE	The energy spectrum entropy in the fault line under high impedance is minimum [12]	<ol style="list-style-type: none"> <li>Calculating the band energy of each line by WPT and the value of energy spectrum entropy using the formula [12]</li> </ol> $H = -\sum_{j=1}^k p_{ji} \ln p_{ji} = -\sum_{j=1}^k [e_j^i(n)]^2 / \sum_{j=1}^k [e_j^i(n)]^2 \ln ([e_j^i(n)]^2 / \sum_{j=1}^k [e_j^i(n)]^2)$ <ol style="list-style-type: none"> <li>The line corresponding to the minimum <math>H</math> is identified as the faulty feeder</li> </ol>	II III
Residual power	$AAD_k$ differentiates high-impedance fault from non-fault cases such as capacitor switching and generator switching [13]	$AAD_k = \sum_{k=1}^n  P_k - P_{k-N} $ [13]	III
Mathematical morphology	The mathematical morphology can be used to distinguish an HIF from other disturbances [14]	An HIF generates a series of non-uniformly distributed spikes over an extended time period, whereas a capacitor switching and load switching generate either a single spike or multiple consecutive spikes over a short time period never longer than one eighth of a cycle	III

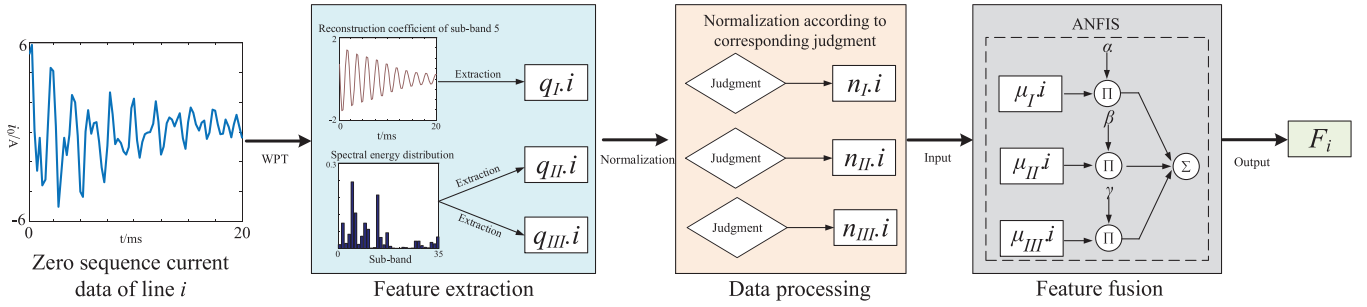


FIGURE 1 Flow framework of the proposed detection method

### 3 | PROPOSED METHOD

#### 3.1 | Proposed multi-feature fusion framework

In this paper, a multi-feature fusion framework based on the three methods is proposed. When a SLG fault occurs, the wavelet packet transform (WPT) [15] is used to extract the fault features of the zero-sequence current based on the corresponding method. Moreover, the extracted fault features are processed according to the characteristics of methods and are fused based on the ANFIS [16]. Finally, the line corresponding to the maximum output of the ANFIS is identified as the faulty feeder. The flow framework of the proposed method is shown in Figure 1, and the list of notations used in this section is summarized in Table 3.

Considering the feeder routine operation in a distribution system, the unique design of the framework, which uses the fault features of each line as the inputs of the ANFIS, enables the proposed method to determine whether a waveform is normal. Consequently, the framework can adapt to the change of distribution network structure.

#### 3.2 | Data pre-processing

When an SLG fault occurs in a distribution system, zero-sequence current of  $N$  lines from the same bus are collected

TABLE 3 List of notations used in this section

Notations	Meaning
$I$	The TCWS method
$II$	The DDCC method
$III$	The WPEE method
$i$	The line $i$
$q$	The fault component
$n$	The normalised fault component
$\mu$	The fault measure value
$\alpha$	Weight coefficient corresponding to method $I$
$\beta$	Weight coefficient corresponding to method $II$
$\gamma$	Weight coefficient corresponding to method $III$

in a relay protection device, and the matrix  $Q$  extracted using the three detection methods is as follows:

$$Q = \begin{bmatrix} q_{I.1} & q_{I.2} & \dots & q_{I.n} \\ q_{II.1} & q_{II.2} & \dots & q_{II.n} \\ q_{III.1} & q_{III.2} & \dots & q_{III.n} \end{bmatrix}. \quad (1)$$

Considering the electrical connection between the feeders on the same bus, the correlation of feeders is essential for the identification of a fault line. On the one hand, the absolute value of fault features extracted using the same detection methods cannot be employed to determine the faulty feeder due to changes in the value in different fault conditions, whereas the relative values of the fault features based on the same method can be employed. Thus, it is necessary to normalise the features of all the lines extracted using the same method, and the relative criterion value of each line is calculated using (2).

$$n.i = \frac{q.i - \min(q)}{\max(q) - \min(q)}, \quad (2)$$

where  $q$  represents the fault features of all the lines extracted using the same method,  $q.i$  represents the fault feature of line  $i$  extracted using the corresponding method, and  $n.i$  represents the normalised fault feature of line  $i$  extracted using the corresponding method.

On the other hand, the absolute value of the fault features also reflects the fault degree to a certain extent, whereas the normalised relative value loses the absolute size of the original data and has a negative effect on the identification of a faulty line under unfavourable conditions. Therefore, it is necessary to set some thresholds for raw data before normalisation. If the threshold is satisfied, the data will be normalised according to (2) directly. Otherwise, the data should be processed according to the corresponding methods. The data processing process is shown in Figure 2.

Considering the different characteristics of the three faulted line detection methods, different normalisation methods should be employed during the data processing process. Ideally, the value extracted using the TCWS method after the occurrence of fault is less than 0 in the fault line and is usually minimum, whereas it is greater than 0 in the non-fault line. Therefore,

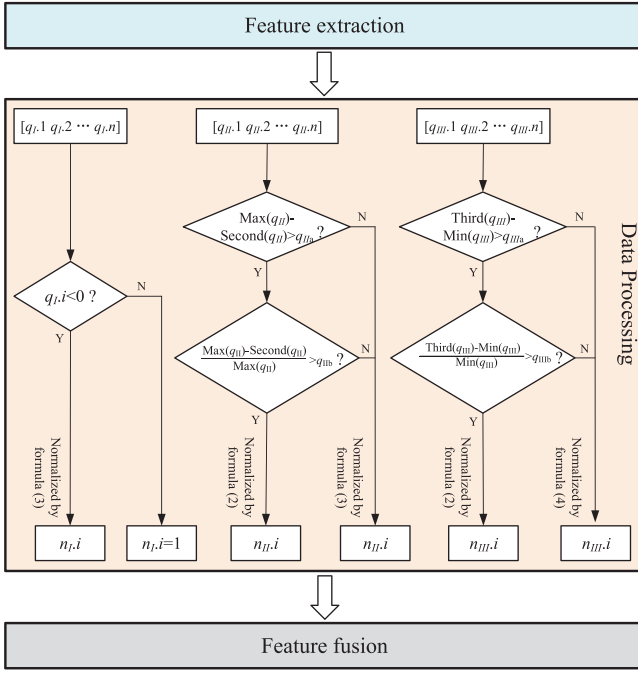


FIGURE 2 Data processing

the normalised values are calculated using (3) and are mapped to the range of  $[0, 0.5]$  when the values extracted using the TCWS method are less than 0; otherwise, they are forced to 1.

$$n_{i,i} = 0.5 \times \frac{q_{i,i} - \min(q)}{\max(q) - \min(q)}. \quad (3)$$

For the DDCC method, the DDCC in the faulted line is the largest, whereas the component is almost 0 in the sound line. Considering the noise and measurement error in the operation of distribution systems, the maximum and secondary maximum values of all the lines extracted using the DDCC method are compared after setting the absolute and relative thresholds. If the thresholds are satisfied, the normalised values extracted using the DDCC method are calculated using (2); otherwise, they are calculated using (3).

For the values extracted using the WPEE method, there are evident differences between the faulted line and the sound line under high-impedance grounding. The value is generally the smallest in the fault line, whereas it is relatively large in the sound line. Considering the difference in the distribution of the values, the minimum and third small values extracted using the WPEE method are selected for comparison by setting the absolute and relative thresholds. If the thresholds are satisfied, the normalised values extracted using the WPEE method are calculated using (2); otherwise, they are calculated using (4).

$$n_{i,i} = 0.5 \times \frac{q_{i,i} - \min(q)}{\max(q) - \min(q)} + 0.5. \quad (4)$$

The final normalised matrix  $N$  is as follows:

$$N = \begin{bmatrix} n_{I,1} & n_{I,2} & \dots & n_{I,n} \\ n_{II,1} & n_{II,2} & \dots & n_{II,n} \\ n_{III,1} & n_{III,2} & \dots & n_{III,n} \end{bmatrix}. \quad (5)$$

### 3.3 | Feature fusion

For different faulted line detection methods, the fault measure membership function should be established separately. Therefore, the matrix  $\mu$  transformed from the matrix  $N$  is shown in formula (6).

$$\mu = \begin{bmatrix} \mu_{I,1} & \mu_{I,2} & \dots & \mu_{I,n} \\ \mu_{II,1} & \mu_{II,2} & \dots & \mu_{II,n} \\ \mu_{III,1} & \mu_{III,2} & \dots & \mu_{III,n} \end{bmatrix}. \quad (6)$$

Different weight coefficients  $\alpha, \beta, \gamma$  are given respectively to the three methods, and the comprehensive fault measure value for each line is obtained in (7).

$$[F_1 \ F_2 \ \dots \ F_n] = [\alpha \ \beta \ \gamma] \begin{bmatrix} \mu_{I,1} & \mu_{I,2} & \dots & \mu_{I,n} \\ \mu_{II,1} & \mu_{II,2} & \dots & \mu_{II,n} \\ \mu_{III,1} & \mu_{III,2} & \dots & \mu_{III,n} \end{bmatrix}. \quad (7)$$

Finally, the line corresponding to the maximum value calculated using (7) is identified as the faulty feeder.

However, the selection of the fault measure membership function and weight coefficients in the fuzzy theory [17] depends on human experience and lacks reliability. Therefore, to avoid the shortage of artificial selection, the ANFIS is employed to determine the fault measure membership function and weight coefficients through the self-learning of a neural network.

In this study, the normalised values of each line extracted using the three detection methods are applied as inputs to the ANFIS, and the comprehensive fault measure value of each line is employed as the output. Eventually, the line corresponding to the maximum output of the ANFIS is identified as the faulty feeder.

## 4 | TRAINING ANFIS

### 4.1 | Simulation

In the training set, a model was established in PSCAD to simulate SLG faults in the typical 10-kV distribution system with resonant grounding. During the simulation, the arc suppression coil was 8% overcompensated, and the sampling rate was 4000 Hz. The structure of the simulation model is as shown in Figure 3.

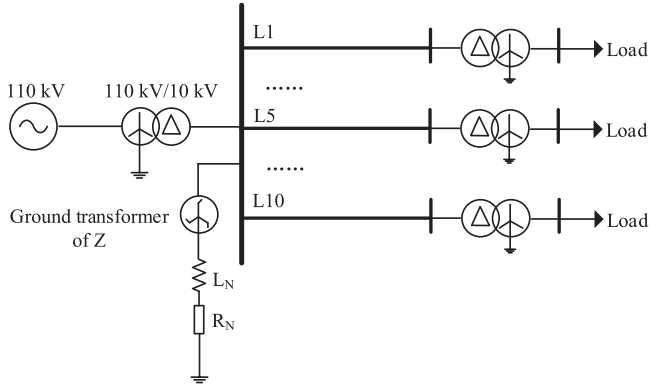


FIGURE 3 Non-effectively grounded distribution network

TABLE 4 Parameters of feeders in the training set

Type	Phase sequence	R ( $\Omega$ /km)	L (mH/km)	C ( $\mu$ F/km)
Overhead line	Positive sequence	0.17	1.21	0.0097
	Zero sequence	0.23	5.48	0.006

The simulation model consisted of ten feeders, and the length of feeders was 1, 3, 7, 15, 20, 25, 35, 40, 44, and 50 km. The type and parameters of feeders are as shown in Table 4.

SLG faults were simulated under different fault conditions, including different faulted feeders, different fault locations, different initial phases, and different grounding resistances. In addition, Gaussian white noise with the signal-to-noise ratio of 50 dB was superposed on the original signal. Different fault conditions are as shown in Table 5.

When training the ANFIS, each input had two membership functions, and the function type employs a Gaussian function. Moreover, the training samples were divided into two categories: the fault line with label 1 and the sound line with label 0. The accuracy of the proposed method and the three detection methods are shown in Table 6. C1 denotes the detection result of the TCWS method, C2 denotes the detection result of the DDCC method, C3 denotes the detection result of the WPEE method, and C denotes the detection result of the proposed method.

TABLE 5 Parameters of fault conditions in the training set

Faulted feeders	Fault location	Initial phases	Grounding resistances	Sample number
L1–L10	10%/	0°–90° per 4.5°	5 $\Omega$ /	8820
	20%/		20 $\Omega$ /	
	40%/		100 $\Omega$ /	
	50%/		500 $\Omega$ /	
	60%/		1000 $\Omega$ /	
	80%		1400 $\Omega$ / 2000 $\Omega$	

TABLE 6 Detection accuracy of methods in the training set

Grounding resistance ( $\Omega$ )	C1 (%)	C2 (%)	C3 (%)	C (%)
5	100	100	44.68	100
20	100	100	52.70	100
100	100	100	78.89	100
500	90.00	100	99.52	100
1000	70.00	58.73	100	100
1400	58.73	16.27	100	100
2000	47.30	0	100	100
Overall accuracy	80.86	67.86	82.26	100

## 4.2 | Discussion

As shown in Table 6, when the grounding resistance is less than 500  $\Omega$ , the TCWS method and the DDCC method have high detection accuracy, whereas the WPEE method has a lower accuracy. When the grounding resistance is equal to 500  $\Omega$ , the DDCC method has the highest accuracy. When the grounding resistance is greater than 500  $\Omega$ , the detection accuracy of the WPEE method also rises to 100%, whereas it gradually decreases when using the TCWS method and the DDCC method.

The above analysis shows that the single detection method has a limitation for the identification of a faulty feeder under different fault conditions. Moreover, the three detection methods have strong complementarity, which is consistent with the previous theoretical analysis. Most importantly, the ANFIS-based method proposed in this paper can adapt to different fault conditions and has an accuracy of 100% for faulted line identification.

## 5 | GENERALISATION ANALYSIS

### 5.1 | Experiments in PSCAD

To validate the detection accuracy in an actual operation of a distribution system, a mode of a 10-kV compensation distribution system composed of 10 feeders was established in PSCAD. The parameters of the feeder lines were different from those in the training set. Moreover, different fault conditions were considered when the feeders were put in operation or moved out of operation, and the noise rose to 30 dB. The type and parameters of lines are as shown in Table 7 and the parameters of different fault conditions are as shown in Table 8.

In addition, a mode of a 10-kV compensation distribution system composed of overhead lines, cable lines, and hybrid lines was established in the following simulations. To verify the strong generalisation ability of the proposed method, the compensation system and ungrounded system composed of three feeders with extremely imbalanced length were also considered.

**TABLE 7** Parameters of the feeder lines in test set

Type	Phase sequence	R ( $\Omega$ /km)	L (mH/km)	C ( $\mu$ F/km)
Overhead line	Positive sequence	0.33	1.31	0.007
	Zero sequence	1.041	3.96	0.004
Cable line	Positive sequence	0.0791	0.2642	0.373
	Zero sequence	0.2273	0.9263	0.166

**TABLE 8** Parameters of fault conditions in test set

Scenarios	Fault location	Initial phases	Grounding resistances	Sample number
1	5%/	$0^\circ$ – $88.2^\circ$	7 $\Omega$ /	4032
2	25%/	per $12.6^\circ$	28 $\Omega$ /	1728
3	45%/		390 $\Omega$ /	1728
	65%/		890 $\Omega$ /	
	85%/		1500 $\Omega$ /	
	95%		2000 $\Omega$	
4	15%/	$0^\circ$ – $90^\circ$		2754
5	35%/	per $1.8^\circ$		2754
6	75%	$0^\circ$ – $88.2^\circ$ per $12.6^\circ$		576

**TABLE 9** Detection accuracy of methods in scenario 1

Method	C1	C2	C3	C
Accuracy	76.76%	60.42%	88.96%	100%

**TABLE 10** Detection accuracy of methods in scenario 2

Method	C1	C2	C3	C
Accuracy	88.77%	58.16%	82.58%	100%

**TABLE 11** Detection accuracy of methods in scenario 3

Method	C1	C2	C3	C
Accuracy	73.21%	72.34%	68.06%	96.41%

**TABLE 12** Detection accuracy of methods in scenario 4

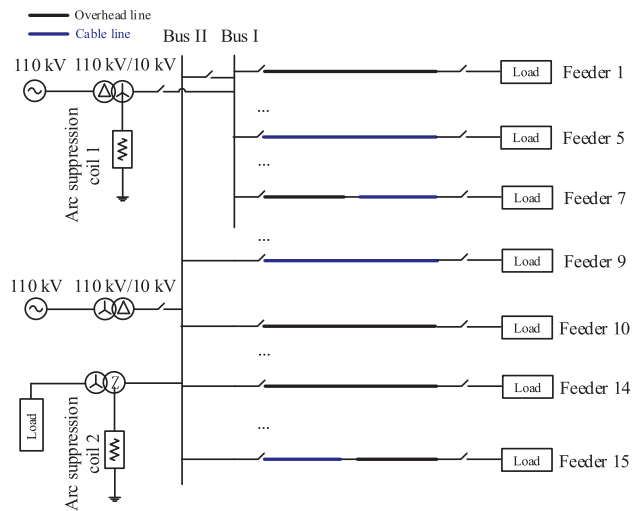
Method	C1	C2	C3	C
Accuracy	56.35%	93.65%	70.66%	99.64%

**TABLE 13** Detection accuracy of methods in scenario 5

Method	C1	C4	C3	C
Accuracy	64.92%	94.84%	85.26%	100%

**TABLE 14** Detection accuracy of methods in scenario 6

PR	C1	C2	C3	C
10%	66.32%	71.53%	88.89%	99.31%
40%	61.11%	71.88%	86.11%	98.96%

**FIGURE 4** RTDS model of a 10-kV distribution system

1. *Feeders put into operation:* When four feeders were put into operation in the test set, the accuracy of the proposed method and the three detection methods are shown in Table 9. The length of the new feeders was 5, 10, 23, and 39 km, and the overcompensation degree increased to 12% in simulation.

As shown in Table 9, the ANFIS-based method does not need to be retrained and has 100% accuracy for identification when the four feeders are put into operation. Therefore, the detection accuracy of the proposed method is not affected when the feeders are put into operation.

2. *Feeders going out of operation:* When the four feeders go out of operation in the test set, the accuracies of the proposed method and the three detection methods are shown in Table 10. The length of the feeders out of operation was 1, 7, 20, and 40 km, and the under-compensation degree was 6% in simulation.

As shown in Table 10, the ANFIS-based method does not need to be retrained and has 100% accuracy for identification when the feeders are put into operation. Therefore, the detection accuracy of the proposed method is not affected when the feeders go out of the operation.

3. *Hybrid distribution system:* Considering the cable lines and hybrid lines used in distribution systems, a mode of a 10-kV hybrid compensation distribution system composed of six feeders was established. The length of the feeders was 5, 15, 25, 35, 45, and 50 km, and the overcompensation degree was changed to 10% in simulation. The detection accuracy is as shown in Table 11.

As shown in Table 11, the trained ANFIS framework in overhead systems can be directly applied to a hybrid distribution system, and the faulty feeder identification accuracy of the

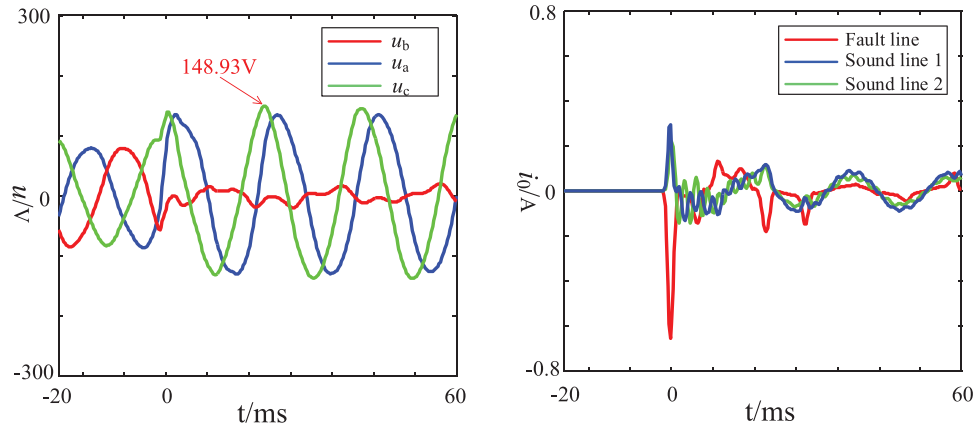


FIGURE 5 Typical waveforms when arc grounding fault occurs

TABLE 15 Fault conditions and detection results

Fault line	Fault phase (°)	Fault resistance ( $\Omega$ )	Harmonic content (%)	Unbalanced voltage (V)	Arc grounding	C1	C2	C3	C
Feeder 1	30	10	0	0	No	✓	✓	✓	✓
	30	10	1	0	No	✓	✓	✓	✓
	30	10	6	0	No	✓	✓	✓	✓
	123	10	0	0	Yes	✓	✓	✓	✓
	150	10	0	2.68	No	✓	✓	×	✓
	150	10	0	5.67	No	✓	✓	×	✓
	150	240	0	0	No	×	×	✓	✓
	243	10	0	0	Yes	✓	✓	×	✓
	330	10	0	5.67	No	✓	✓	✓	✓
	330	240	0	0	No	×	✓	✓	✓
Feeder 5	330	1000	0	0	No	×	×	✓	✓
	90	10	0	0	No	✓	✓	×	✓
	123	10	0	0	Yes	✓	✓	✓	✓
	150	1.1	0	0	No	✓	✓	×	✓
	150	3.3	0	0	No	✓	✓	×	✓
	150	7.7	0	0	No	✓	✓	×	✓
	150	1000	0	0	No	✓	×	✓	✓
	270	10	0	0	No	✓	✓	×	✓
	330	1.8	0	0	No	×	✓	✓	✓
	330	10	0	2.68	No	×	✓	✓	✓
Feeder 7	90	10	0	0	No	✓	✓	×	✓
	123	10	0	0	Yes	✓	✓	×	✓
	270	10	0	0	No	✓	✓	✓	✓
Feeder 9	60	10	0	0	No	✓	✓	✓	✓
	243	10	1	0	No	✓	✓	×	✓
	243	10	6	0	No	✓	✓	✓	✓
Feeder 10	210	10	0	0	No	✓	✓	✓	✓
	210	10	1	0	No	✓	✓	×	✓
	210	10	6	0	No	✓	✓	✓	✓
	270	10	0	0	No	✓	×	✓	✓
	330	10	0	0	No	×	✓	✓	✓



proposed method is higher than that of the three original methods.

4. *Different voltage grade system*: To verify the wide applicability of the proposed method in this paper, the system voltage level was changed, and a compensation distribution system composed of three feeders with an extremely imbalanced length was established in PSCAD. The length of the feeders was 5, 20, and 80 km, and the overcompensation degree was change to 15% in simulation. The detection accuracy is as shown in Table 12.

As shown in Table 12, the extreme structure of the distribution system poses a great challenge to the faulty line detection based on the TCWS method or the WPEE method, whereas the DDCC method has a higher detection accuracy. The feature fusion of the three methods based on the ANFIS achieves complementary advantages and exhibits the highest accuracy. Therefore, the detection accuracy of the proposed method is not affected by the structure of the distribution system.

5. *Ungrounded system*: Considering different neutral grounding modes, a mode of a 35-kV ungrounded system with three overhead lines was established. The length of the feeders was also extremely imbalanced and was the same as those in scenario 4).

As there was almost no DDCC in the ungrounded system, the fundamental waveform amplitude method was employed instead of the DDCC method. Moreover, the ANFIS-based method does not need retraining because the fundamental waveform amplitude method also selects the line corresponding to the maximum value as the faulty feeder. The detection accuracy is as shown in Table 13, and C4 denotes the detection result of the fundamental waveform amplitude method.

As shown in Table 13, the ANFIS-based method has an accuracy of 100% for identification in an ungrounded system. Therefore, the ANFIS-based method proposed for a compensation system can be applied for the identification of faulted lines in ungrounded systems.

6. *Distributed generation*: Considering the effect of distributed generation (DG), a mode of a 10-kV compensation system with DG was established. The length of overhead lines was 20, 30, 40 and 50 km, and DG was connected to the 30 km feeder. The detection accuracy of methods under different penetration rate (PR) are as shown in Table 14.

As shown in Table 14, the detection accuracy of the ANFIS-based method drops slightly from 99.31% to 98.96% when PR rises sharply from 10% to 40%, and consequently, distribution systems with DG have little impact on the detection accuracy of the proposed method.

In summary, the trained ANFIS-based method can adapt to the operation of feeders, hybrid systems, different voltage grade systems, different neutral grounding modes and distribution systems with DG. The PSCAD simulation results demonstrate that the proposed method has a superior generalisation ability.

## 5.2 | Experiments in RTDS

To verify the application in engineering, a model was established in RSCAD to simulate SLG faults in the HIL tests of RTDS. The power amplifiers made by PONOVO was employed to convert digital signal into analog signal. The analog signal was added to the relay protection device, which sends trip signals to the breaker. The data of zero-sequence voltage and current was collected by fault recorder. The structure of the RTDS model is as shown in Figure 4.

Considering the arc grounding events when a SLG fault occurs, arc grounding faults were simulated in several cases and the typical voltage and zero-sequence current waveforms are shown in Figure 5.

As shown in Figure 5, the non-fault phase voltage  $u_c$  rises to 148.93 V and is 2.58 times the normal operating phase voltage, which greatly affects the insulation of electrical equipment. Meanwhile, the arc grounding current has noticeable distortions and presents a challenge to the fault line detection.

Different fault conditions and the corresponding detection results in RTDS are as shown in Table 15.

As shown in Table 15, the trained ANFIS-based method in PSCAD can be directly applied to more demanding and realistic engineering environments in RTDS. Moreover, the proposed method is free from the influence of harmonic content, unbalanced voltage, and arc grounding, which are not considered in the training set. Therefore, the proposed method has a strong generalisation ability and is valuable in engineering applications.

## 6 | CONCLUSION

Based on the classification of SLG faults in distribution systems with resonant grounding, this study analysed the adaptability of the existing faulted line detection methods under different fault types. Subsequently, three kinds of fault features were extracted using the TCWS method, DDCC method, and WPEE method, which can adapt to all fault types and have complementarity. To improve the generalisation ability of the detection methods, the corresponding normalisation methods and a unique structure design of ANFIS are proposed. The PSCAD and RTDS experiments in different distribution systems confirmed the rationality of method selection and its superior generalisation ability.

### ACKNOWLEDGEMENT

This work was funded by Science and Technology Project of State Grid Corporation of China 'Research on Fault Diagnosis and Self-Organization Control for Distribution Network with High Penetration DER integration'.

### REFERENCES

1. Hanninen, S., et al.: Characteristics of earth faults in power systems with a compensated or an unearthed neutral. In: 14th International Conference and Exhibition on Electricity Distribution. Part 1. Contributions (IEE Conf. Publ. No. 438), Birmingham, pp. 16/1–16/5 (1997)
2. Zhu, K., et al.: Controlled closing of PT delta winding for identifying faulted lines. IEEE Trans. Power Delivery 26(1), 79–86 (2011)

3. Yuan, S., et al.: Analysis and comparison of several fault line selective methods in small current grounding power system. In: 2008 China International Conference on Electricity Distribution, Guangzhou, pp. 1–7 (2008)
4. Dong, X., Shi, S.: Identifying single-phase-to-ground fault feeder in neutral noneffectively grounded distribution system using wavelet transform. *IEEE Trans. Power Delivery* 23(4), 1829–1837 (2008)
5. Ji, T., et al.: Study on fault line detection based on genetic artificial neural network in compensated distribution system. In: 2006 IEEE International Conference on Information Acquisition, Weihai, pp. 1427–1431 (2006)
6. Liu, J., et al.: Research on multi-criteria fusion strategy of fault line selection in distribution network based on fuzzy theory. *Electrical Engineering* 10, 23–30 (2016)
7. Shu, H., et al.: Integration of multi-algorithm for single-phase fault detection in distribution system with arc suppression coil grounding using extenics. In: 2008 IEEE International Conference on Electric Utility Deregulation and Restructuring and Power Technologies, Nanjing, pp. 2111–2115 (2008)
8. Elkalashy, N., et al.: Bayesian selectivity technique for earth fault protection in medium-voltage networks. *IEEE Trans. Power Delivery* 25(4), 2234–2245 (2010)
9. Du, Y., et al.: Single line-to-ground faulted line detection of distribution systems with resonant grounding based on feature fusion framework. *IEEE Trans. Power Delivery* 34(4), 1766–1775 (2019)
10. Xue, Y., et al.: Transient equivalent circuit and transient analysis of single-phase earth fault in arc suppression coil grounded system. *Proceedings of the CSEE* 35(22), 5703–5714 (2015)
11. Tian, S., et al.: A new method of fault location for 35KV distribution network based on the equivalent load to ground. in: 2011 Chinese Control and Decision Conference (CCDC), Mianyang, pp. 87–91 (2011)
12. Qin, H., Li, T.: High impedance faultline selection method for resonant grounding system based on wavelet packet analysis. In: 2018 China International Conference on Electricity Distribution (CICED), Tianjin, pp. 1174–1179 (2018)
13. Kujur, A., Biswal, T.: Detection of high impedance fault in distribution system considering distributed generation. In: 2017 International Conference on Innovative Mechanisms for Industry Applications (ICIMIA), Bangalore, pp. 406–410 (2017)
14. Gautam, S., Brahma, S., Detection of high impedance fault in power distribution systems using mathematical morphology. *IEEE Trans. Power Syst.* 28(2), 1226–1234 (2013)
15. Coifman, R., Wickerhauser, M., Entropy-based algorithms for best basis selection. *IEEE Trans. Inf. Theory* 38(2), 713–718 (1992)
16. Jang, J.: ANFIS: Adaptive-network-based fuzzy inference system. *IEEE Trans. Syst. Man Cybern.* 23(3), 665–685 (1993)
17. Zadeh, L.: Outline of a new approach to the analysis of complex systems and decision processes. *IEEE Trans. Syst. Man Cybern.* SMC-3(1), 28–44 (1973)

**How to cite this article:** Yuan J, Jiao Z, Feng G, Chen M, Xu M. Study on fault line detection methods based on multi-feature fusion in distribution systems. *IET Gener Transm Distrib.* 2020;1–10.  
<https://doi.org/10.1049/gtd2.12064>